Information-Centric Offloading in Cellular Networks with Coordinated Device-to-Device Communication

Asma Afzal, Syed Ali Raza Zaidi, Des McLernon and Mounir Ghogho

arXiv:1608.03429v1 [cs.NI] 11 Aug 2016

Abstract

In this paper, we develop a comprehensive analytical framework for cache enabled cellular networks overlaid with coordinated device-to-device (D2D) communication. We follow an approach similar to LTE Direct, where the base station (BS) is responsible for establishing D2D links. We consider that an arbitrary requesting user is offloaded to D2D mode to communicate with one of its *'k'* closest D2D helpers within the macrocell subject to content availability and helper selection scheme. We consider two different D2D helper selection schemes: 1) uniform selection (US), where the D2D helper is selected uniformly and 2) nearest selection (NS), where the nearest helper possessing the content is selected. Employing tools from stochastic geometry, we model the locations of BSs and D2D helpers using independent homogeneous Poisson point processes (HPPPs). We characterize the D2D mode probability of an arbitrary user for both the NS and US schemes. The distribution of the distance between an arbitrary user and its *i*th neighboring D2D helper within the macrocell is derived using disk approximation for the Voronoi cell, which is shown to be reasonably accurate. We fully characterize the overall coverage probability and the average ergodic rate of an arbitrary user requesting a particular content. We show that significant performance gains can be achieved compared to conventional cellular communication under both the NS and US schemes when popular contents are requested and NS scheme always outperforms the US scheme. Our analysis reveals an interesting trade off between the performance metrics and the number of candidate D2D helpers *'k'*. We conclude that enhancing D2D opportunities for the users does not always result in better performance and the network parameters have to be carefully tuned to harness maximum gains.

The authors are with the School of Electronic and Electrical Engineering, University of Leeds, United Kingdom. M. Ghogho is also affliated with the University of Rabat, Morocco.

Email: {elaaf, s.a.zaidi, d.c.mclernon, m.ghogho}@leeds.ac.uk

I. INTRODUCTION

Ubiquitous devices such as smart phones and tablets have fueled the demand for data intensive applications, including ultra high-definition video streaming, social networking and e-gaming. This puts significant pressure on the traditional cellular networks, which are not designed to support such high data rates and reliability requirements. As a consequence, current research on fifth generation (5G) wireless networks is geared towards developing intelligent ways of data dissemination by deviating from the traditional host centric network architecture to a more versatile information centric architecture.

Caching in the IP networks has already proved to be a promising way to reduce the overhead of backhaul communication. Borrowing from these principles, caching at the edge of the cellular networks potentially reduces the backhaul access cost in terms of capacity, latency and energy consumption by turning memory into bandwidth [1]. Recent observations have indicated that the data traffic consists of a lot of duplications of multimedia content requested by various users in the same vicinity [2]. Therefore, users can leverage this trend to their advantage by accessing information pre-downloaded by their neighboring users using Direct device-to-device (D2D) communication. D2D communication is a promising technique to improve the coverage and throughput of cellular networks [3]. Mobile users in close physical proximity can exchange popular files without the intervention of the base station (BS). This not only offloads the burden of duplicate transmissions from the BS, but it also provides higher rates due to short range D2D communication [4]. Several techniques have been proposed to materialize the concept of integrating D2D communication with cellular networks. The major design questions are: Should D2D communication operate in the cellular uplink or downlink, licensed spectrum or unlicensed spectrum, and in the licensed spectrum should it be underlay or overlay, coordinated by the BS or uncoordinated? In this paper, we focus on coordinated in-band overlay D2D communication in the cellular downlink, where a macro base station (MBS) establishes, manages and arbitrates a D2D connection [5]. The reader is referred to a detailed discussion of the other D2D implementation techniques in [6] and the references therein.

So, the novelty of this paper is as follows. We propose a new information-centric offloading mechanism, whereby the MBS maintains a record of the previously downloaded contents by the users in its long term-coverage region. Based on this information, the MBS schedules a D2D

link between a user and one of its k neighboring D2D helpers subject to the content availability and helper selection scheme. These D2D helper devices can be considered as users which are not receiving any data form the MBS in the current radio frame and can transmit their data. We consider two different helper selection schemes, namely, 1) nearest helper selection (NS): where the MBS selects the D2D helper closest to the user possessing the requested content and 2) uniform selection (US): where the MBS uniformly selects a D2D helper first and checks for content availability later. The estimation of a user's location is much accurate thanks to the in-built GPS and location apps in smart phones. Fig. 1 displays a simple example of the scenario under consideration. The MBS examines its records for the arrived content requests and schedules possible D2D transmissions. Here, User#1 is served by its second nearest D2D helper, while User#2 is served by the MBS as none of its k neighboring helpers have the content.

We analyze such a system with the help of stochastic geometry to quantify the performance improvement compared to conventional and cache enabled single tier cellular networks. Stochastic geometry has recently emerged as a powerful tool to accurately analyze the performance of large scale cellular networks [7]. We make use of the Poisson point process (PPP) assumption in modeling the locations of the MBSs and D2D to derive tractable expressions for various performance metrics.

The main contributions of this article are summarized as follows.

- For the information-centric offloading paradigm, we consider that both the D2D helpers and BSs are equipped with caches and an arbitrary user requests a certain content based on its popularity. It is important to note that in this work, we focus on devising efficient data dissemination techniques for a given content placement strategy. Based on the content placement strategy, helper selection schemes and other caching parameters, we derive expressions for the probability that an arbitrary user is served in D2D mode for both the NS and US schemes. We obtain bounds on this probability and study its behavior as the number of candidate helpers k grows.
- With the help of our stochastic geometry framework, we derive the distribution of distance between an arbitrary user and its ith nearest D2D helper within the cell using a disk approximation for a Voronoi cell. We show that this approximation is fairly accurate for various values of i and compare it with the distribution of distance between the requesting user and its ith nearest D2D helper not necessarily present inside the cell. We investigate

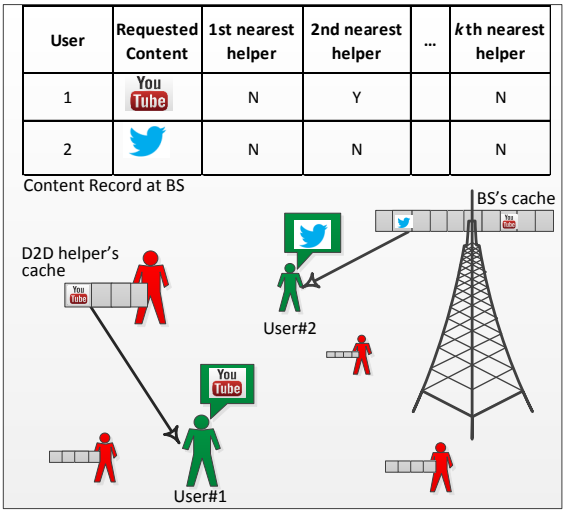

Figure 1: Illustration of cache-enabled coordinated D2D network. The MBS pairs the requesting users with one of their k neighbors depending on the content availability and helper selection scheme. If none of the k neighbors have the content, the MBS serves the user itself.

the conditions in which our derived distribution reduces to the unconstrained case.

- We characterize the coverage probability for individual D2D links and the probability that an arbitrary user is in coverage when it requests a particular content and operates in D2D mode with the NS and US schemes. We also validate our results with network simulations.
- We explore the two important performance metrics, including the overall coverage probability and the average rate experienced by an arbitrary user requesting a particular content c. We show that there exists an optimal number of candidate D2D helpers k which maximize the overall coverage and the average rate. The optimal k maximizing the coverage probability is independent of caching parameters or the requested content and only depends on the network parameters. However, that is not the case for the optimal k maximizing the average rate. We also show that high performance gains can be harnessed compared to conventional cellular communication when the most popular contents are requested.

A. Related Work

Characterization of the performance of caching enabled cellular networks has been widely studied in [8]–[10] to name a few. However, all these works make use of the simplistic protocol model, where outage occurs if the intended receiver is at a distance greater than a fixed distance from the transmitter or there is another interfering transmitter present within the range of the receiver. The other approach, which makes use of the physical model, is where the outage occurs on the basis of the received signal-to-interference-and-noise ratio (SINR).

Stochastic geometry has been widely applied to analyze the physical layer metrics of the large scale wireless networks. For the case of cache enabled cellular networks, the dynamics of content popularity, propagation conditions and spatial locations are employed in [11]–[18] to quantify the performance gains. The analysis of rate and energy efficiency for single-tier cache enabled cellular networks is carried out in [14] and [16]. An optimal content placement strategy is devised in [16], which maximizes the rate coverage and the energy efficiency of the single-tier cellular networks. The authors in [17] and [18] consider clustered D2D networks, which operate in isolation from the underlying cellular network. In [17], the authors consider clustering to mimic spatial content locality without explicitly considering content popularity and storage. It is assumed that for a user in a given cluster, there will always be a device in that cluster with the requested content i.e., a D2D wireless link is always established. Whereas, the authors in [18] consider D2D devices with caching and a Zipf type content popularity distribution. Here, clustering is considered so that there are finite transmissions within the cluster multiplexed in time as in TDMA and one link is active at a given time. In [15], the analysis is carried out with different D2D transmitter selection schemes, but this work makes use of the same clustered users model as in [17]. All these works do not take into account the coexistence of D2D communication with cellular networks and that if D2D communication is infeasible, the users can communicate with the MBS.

For the case of multi-tier analysis with caching, the authors in [12] and [13] consider distributed caching, where a user can access data from the caches of multiple small base stations (SBSs) inside a cell. However, in case of the content availability in any one of the SBSs within the cell, the user is always served by its nearest SBS assuming that the content transfer takes place among the SBSs. This is different from our case as we cannot expect such level of cooperation

between D2D helpers and need explicit characterization of the distances of the individual D2D helpers from the arbitrary user.

The selection of cellular and D2D modes is studied for the uplink in [19] and [20]. In [19], the decision to transmit in D2D mode is based on the distance to the receiver uniformly placed around the D2D transmitter, while in [20], it also depends on the distance from the BS. Both of these approaches ignore the aspects of content availability, popularity and storage.

Various content replacement policies and storage techniques are studied in [21]–[23]. [22] shows how updating a cache by evicting the least recently used (LRU) content could provide performance gains. It is shown that least frequently used (LFU) policy outperforms LRU in [24]. [23] explores how caches could be updated by exploiting social ties between users using transfer learning approach. [21] proposes coded caching for delay sensitive applications. In [25] and [26], the authors explore the effect of geometric placement of caches to devise optimal content placement strategies. A simpler, fixed-caching approach is adopted in [14], [18], [27] and [13], where the cache is not updated and the stored files are simply considered to follow the popularity distribution.

The remainder of this paper is organized as follows: Section II describes the spatial setup, signal propagation, content popularity and caching models, and the information-centric offloading paradigm for both the NS and US schemes. Section IV provides the derivation of the distance between an arbitrary user and its ith nearest D2D helper within the cell. The distribution of this distance is then used to characterize the overall coverage and the average rate for the NS and US schemes in Section V. Section VI discusses the results and validates our analysis with network simulations. Section VII concludes the paper.

II. System Model

We consider a cellular downlink (DL) scenario of MBSs overlaid with D2D helpers. The MBS schedules a requesting user with one of its neighboring D2D helpers inside the cell if the helper has the requested file. The network description and the key assumptions now follow.

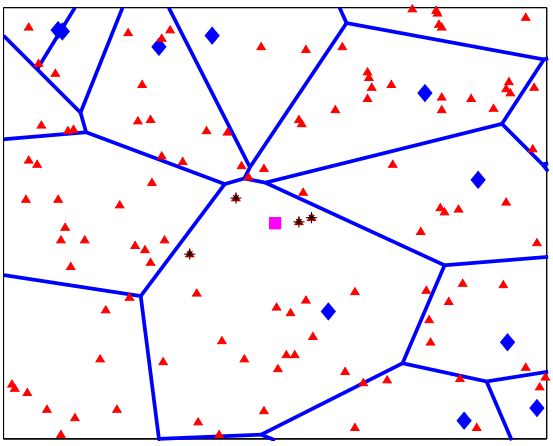

Figure 2: Spatial model of the network. MBSs are depicted by blue, filled diamonds; D2D helpers by red, filled triangles; and the requesting user by a filled magenta square. The k candidate D2D helpers for D2D communication are marked with black asterisks (here, $k = 4$) and $\lambda_d = 10\lambda_m$.

A. *Spatial Model*

According to the theory of HPPPs, the distribution of $\Phi(\mathcal{A})$, where $\mathcal{A}$ is a bounded borel set in $\mathbb{R}^2$, is given as

$$\mathbb{P}[\Phi(\mathcal{A}) = n] = \frac{(\lambda\mu(\mathcal{A}))^n}{n!}\exp\left(-\lambda\mu(\mathcal{A})\right), \tag{1}$$

where λ is the intensity of the HPPP and $\mu(\mathcal{A}) = \int_{\mathcal{A}} dx$ is the Lebesgue measure on $\mathbb{R}^2$. For a disc of radius r in $\mathbb{R}^2$, $\mu(\mathcal{A}) = \pi r^2$. We consider that the MBSs, D2D helpers and the requesting users are distributed according to independent HPPPs Φ_m, Φ_d, and Φ_u with intensities λ_m, λ_d and λ_u respectively, where $\lambda_u, \lambda_d \gg \lambda_m$. The requesting users are associated to the nearest MBS and the user association region is defined as

$$\begin{aligned}\mathcal{S}_i \overset{def}{=} \; & x \in \mathbb{R}^2 \; : \; \|y_i - x\| < \|y_j - x\|, \\ & \forall\, y_i, y_j \in \Phi_m, i \neq j,\end{aligned} \tag{2}$$

where $\mathcal{S}_i$ represents a Voronoi cell of the MBS located at $y_i \in \Phi_m$[1]. Without any loss of generality, we measure performance at the requesting user located at the origin. This follows

[1]We use the same notation to denote the the node itself and its distance to the origin.

from the palm distribution of HPPPs and Slivnyak's theorem [28]. The MBS selects one of the k closest D2D helpers and establishes a D2D link (the selection process is described in detail in the next section). A realization of the spatial setup is shown in Fig. 2.

B. Propagation Model and Spectrum Access

We assume that both the cellular and D2D links experience channel impairments including path loss and small-scale Rayleigh fading. The power received at the origin from the MBS/ D2D helper located at $y \in \Phi_n, n = \{m, d\}$ is given as $P_n h\, y^{-\alpha}$, where P_m and P_d are the transmit powers of the MBS and D2D helper respectively, α represents the path loss exponent ranging between 2 and 5 and h is the channel power. We assume that h is a unit-mean exponential RV representing the squared-envelope of Rayleigh fading.

We consider an in-band overlay spectrum access strategy, where fixed bandwidths W_m and W_d are allocated for cellular and D2D communication respectively. We assume that there is universal frequency reuse across the network, but the number of resource blocks is greater than the number of users within the cell and hence, there is no intra-cell interference.

C. Content Popularity and Caching Model

The performance of caching is crucially determined by the content popularity distribution. It has been observed that the popularity of data follows a Zipf popularity distribution where, the popularity of the cth content is proportional to the inverse of c^{ζ} for some real, positive, skewness parameter ζ. It is mathematically represented as

$$pop(c) = \rho c^{-\zeta} \;\; 1 \leq c \leq L, \tag{3}$$

where $\rho = \left(\sum_{l=1}^{L} l^{-\zeta}\right)^{-1}$ is the distribution normalizing factor and L is the file library size. $\zeta = 0$ corresponds to uniform popularity while a higher value of ζ results in a more skewed distribution. Empirical evidence shows that the value for ζ exists between 0.6 to 0.8 for different content types including web, file sharing, user generated content (UGC) and video on demand (VoD) [24]. We consider that the MBS and the D2D helpers are equipped with caches of sizes C_m and C_d respectively. All files are considered to have a unit size. Our analysis can easily be extended for variable file sizes as each memory slot will then contain a chunk of a file. We further assume that user requests follow the independent reference model (IRM) as introduced in

[24]. According to the IRM, the user requests for a file in the library are independently generated following the popularity distribution and there is no spatio-temporal locality, i.e. identical contents have the same popularity in space and time [12].

1) Content Placement: We consider that the MBS stores C_m most popular files in its cache. The MBS caches the most popular contents, which coincides with the least frequently used (LFU) content placement strategy. Because the content popularity does not rapidly change in time, LFU placement is shown to be well-suited for the MBS. The cellular hit rate for content c, which is the probability that the content c is present in the MBS's cache is given as

$$h_m(c) = \mathbb{I}_{c \leq C_m}, \tag{4}$$

where $\mathbb{I}_{c \leq C_m}$ is an indicator variable taking the value 1 when $c = \{1, .., C_m\}$ and 0 otherwise.

When there is a set of candidate D2D helpers which can serve a single user, the LFU placement for all D2D helpers is not optimal. Such a scenario requires a collaborative content placement strategy which takes into account the number and the locations of the D2D helpers [25], [26]. Investigating the optimal content placement strategy for D2D helpers for this network setup is a research issue in itself and left for future work. We consider a sub-optimal but tractable content placement strategy for the D2D helpers to quantify the advantage of employing content-centric offloading on D2D mode. We consider that each D2D helper stores the content c in each memory slot independently according to the popularity distribution $pop(c)$. The D2D hit rate for content c, is then given as

$$\begin{aligned} h_d(c) &= 1 - \mathbb{P}[\text{Content } c \text{ not present in } C_d \text{ slots}] \\ &= 1 - [1 - \rho c^{-\zeta}]^{C_d}. \end{aligned} \tag{5}$$

III. Information-Centric Offloading

We assume that for a typical user requesting content c, the MBS will examine the contents of up to k neighboring D2D helpers within the cell. The selection of the D2D helper depends on the helper selection scheme and the popularity of the requested content itself. The following proposition gives the probability for the selection of a particular D2D helper.

Proposition 1. *The probability that an arbitrary user requesting content 'c' is served by the ith*

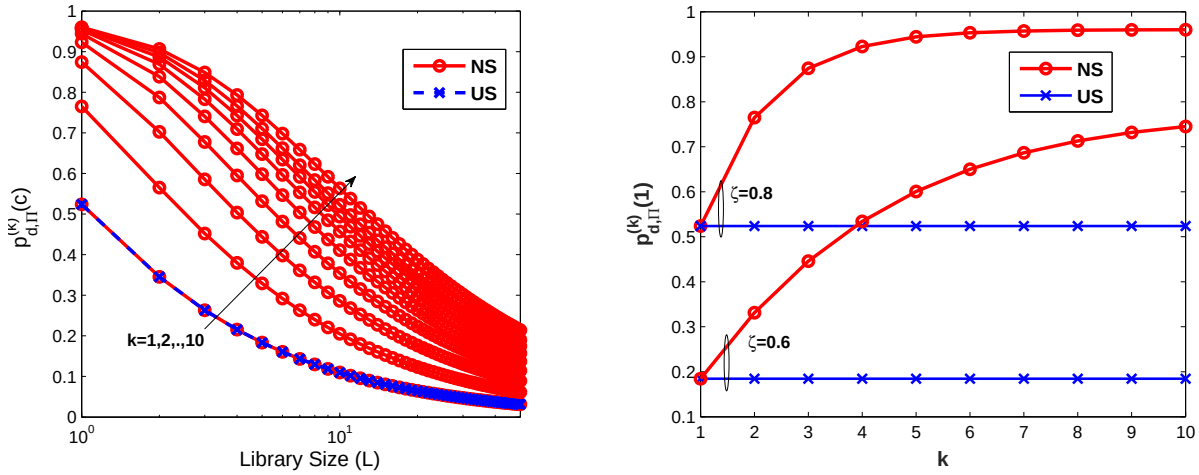

(a) (b)

Figure 3: Effect of helper selection schemes, requested contents, k and ζ on the probability of D2D and cellular modes.

nearest D2D helper within the cell under NS and US schemes is given by

$$p_{d,NS}^{(k)}(i,c) = \frac{343}{30}\sqrt{\frac{14}{\pi}}\frac{\Gamma(i+3.5)\,\eta_d^i\,{}_2F_1\left(1,i+3.5;i+1;\frac{\eta_d}{(\eta_d+3.5)}\right)}{i!\,(\eta_D+3.5)^{i+3.5}}\left(1-h_d(c)\right)^{i-1}h_d(c), \quad (6)$$

and

$$p_{d,US}^{(k)}(i,c) = h_d(c)\left[\frac{343}{30}\sqrt{\frac{14}{\pi}}\frac{\Gamma(k+4.5)\,\eta_d^{k+1}\,{}_2F_1\left(1,k+4.5;k+2;\frac{\eta_d}{(\eta_d+3.5)}\right)}{k(k+1)!\,(\eta_d+3.5)^{k+4.5}} + \sum_{j=0}^{k-i}\frac{3.5^{3.5}\Gamma(i+j+3.5)\eta_d^{i+j}}{\Gamma(3.5)\,(i+j)\,(i+j)!\,(\eta_d+3.5)^{i+j+3.5}}\right] \quad (7)$$

respectively, where $\eta_d = \lambda_d/\lambda_m$, $i = \{1,..k\}$, $\Gamma(a)$ *is the complete Gamma function and* ${}_2F_1\,(a,b;c;x)$ *is the generalized hypergeometric function.*

Proof: For the user to be served by the ith nearest D2D helper, there must be at least i D2D helpers inside the cell. In the NS scheme, the user is served by the ith helper if no closer helper has the requested content. This implies

$$p_{d,NS}^{(k)}(i,c) = \mathbb{P}\left[N_d \geqslant i\right]\left(1-h_d(c)\right)^{i-1}h_d(c), \quad (8)$$

where N_d is the number of D2D helpers in a Voronoi cell whose probability mass function is given as [29]

$$\mathbb{P}\left[N_d = j\right] = \frac{3.5^{3.5}\Gamma(j+3.5)(\lambda_d/\lambda_m)^j}{\Gamma(3.5)\, i!\, (\lambda_d/\lambda_m + 3.5)^{i+3.5}}. \tag{9}$$

This implies $\mathbb{P}\left[N_d \geqslant i\right] = 1 - \sum_{j=0}^{i-1} \mathbb{P}\left[N_d = j\right]$. Substituting this expression in (8) gives (6).

For the US scheme, the user is served by the ith helper if it is uniformly selected and has the requested content. This implies

$$p_{d,US}^{(k)}(i,c) = h_d(c)\left[\frac{1}{k}\mathbb{P}\left[N_d > k\right] + \sum_{j=0}^{k-i}\frac{1}{i+j}\mathbb{P}\left[N_d = i+j\right]\right], \tag{10}$$

Substituting the expressions for $\mathbb{P}\left[N_d > k\right]$ and $\mathbb{P}\left[N_d = i+j\right]$ completes the proof. ■

The probability that an arbitrary user is served in D2D mode under NS and US schemes is a straightforward summation of $p_{d,NS}^{(k)}(i,c)$ and $p_{d,US}^{(k)}(i,c)$ over $i = \{1, 2.., k\}$. This gives

$$p_{d,NS}^{(k)}(c) = \sum_{i=1}^{k} p_{d,NS}^{(k)}(i,c), \tag{11}$$

and

$$p_{d,US}^{(k)}(c) = p_{d,US}^{(1)}(c) = h_d(c)\left[1 - (1 + 3.5^{-1}\eta_d)^{-3.5}\right]. \tag{12}$$

It is interesting to note that in case of the US scheme, $p_{d,US}^{(k)}(c)$ is independent of k. This is because the probability of the D2D mode depends on the contents of only one helper selected at random.

Corollary 1. *The bounds on $p_{d,\Pi}^{(k)}(i,c), \Pi = \{NS, US\}$ with respect to η_d are given as*

$$p_{d,NS}^{(k)}(i,c) \leq \left(1 - h_d(c)\right)^{i-1} h_d(c) \tag{13}$$

and

$$p_{d,US}^{(k)}(i,c) \leq \frac{1}{k} h_d(c) \tag{14}$$

where the equalities hold when $\lambda_d \gg \lambda_m$ and $\eta_d \to \infty$.

Proof: As $\eta_d \to \infty$, $\mathbb{P}\left[N_d \geqslant k\right] \to 1$, i.e. there are definitely at least k D2D helpers within the cell and (8) reduces to $\left(1 - h_d(c)\right)^{i-1} h_d(c)$. It can be easily seen from (10) that as $\mathbb{P}\left[N_d \geqslant k\right] \to 1$, $\mathbb{P}\left[N_d = i+j\right] \to 0$, where $i + j < k$. Hence, $p_{d,US}^{(k)}(c)$ reduces to $h_d(c)$. ■

Before moving on to further analysis, we explore the behavior of the D2D mode probability in Figs. 3a and 3b. The values of the simulation parameters used in plotting the results are listed

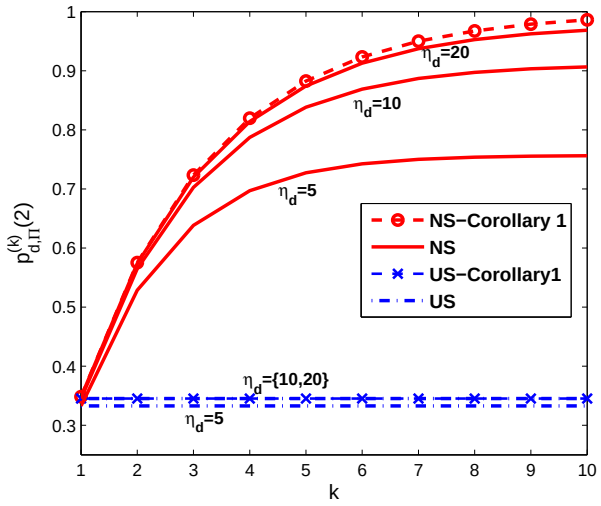

Figure 4: Effect of helper density on D2D mode probability.

further on in Table I unless stated otherwise. We can see that there is a rapid increase in $p_{d,NS}^{(k)}(c)$ initially with the increase in k, but diminishing gains are observed when k is further increased. A sharp decrease in $p_{d,NS}^{(k)}(c)$ is observed as the requested content becomes less popular or the skewness parameter ζ decreases. As established in (12), we see that there is no effect of increasing k on $p_{d,US}^{(k)}(c)$. In Fig. 4, we plot the D2D mode probabilities $p_{d,\Pi}^{(k)}(c) = \sum_{i=1}^{k} p_{d,\Pi}^{(k)}(i,c), \Pi = \{NS, US\}$ using the upper bounds from Corollary 1 and compare them for the actual values of $p_{d,\Pi}^{(k)}(c)$ in (11) and (12). We see that the deviation for the NS scheme becomes large as the value of k increases, but convergence is fast and the bounds are fairly tight for $\eta_d \geq 10$.

IV. Distance to the ith nearest D2D helper within a Macrocell

One of the main contributions of this paper is to characterize the distribution of the distance between the typical user and the ith nearest D2D helper within the macro cell. It is a well-known fact that the distance between the nearest neighbors for a 2-D Poisson process is Rayleigh distributed and this has been widely adopted for the stochastic geometry analysis of cellular networks [19], [20], [14], [30]. In our case, however, the MBS only keeps a record of the files stored in the memory of D2D helpers within its coverage region. Therefore, it can only connect the requesting user with the helpers within its cell. Fig. 2 illustrates that in our spatial setup, the ith nearest D2D helper is not always within the macrocell. Hence, this adds a layer of complexity

to our model as the distance is no longer independent of the geometrical attributes of the cell, including its shape and size.

The distribution of the exact shape and size of a typical Voronoi cell in a 2-D Poisson Voronoi tessellation is still unknown. In their analysis of bivariate Poisson processes in [31], Foss and Zuyev make use of the maximal disk approximation for the Voronoi cell. The maximal disk, B_{max}, is the largest disk centered at the MBS inscribing the Voronoi cell. The exact characterization of the distribution of the radius X of B_{max} is straight forward as it is the probability that there is no other BS at a distance $2x$ from the tagged BS and is expressed as $\mathbb{P}[X \geq 2x] = \exp\left(-4\lambda_m \pi x^2\right)$. This implies

$$f_X(x) = 8\lambda_m \pi x \, \exp(-4\lambda_m \pi x^2). \tag{15}$$

In this work, we utilize the maximal ball approximation for the Voronoi cell to derive the distribution of the distance between the typical user and its ith nearest D2D helper[2]. The following Lemmas provide some useful preliminary results which are necessary conditions for the characterization of the distance distribution.

Lemma 1. *The probability that the typical user lies inside B_{max} is the probability that the radius of B_{max} is greater than the distance between the MBS and typical user. It is a constant value and is equal to*

$$p_{in} = \mathbb{P}\left[X \geq Y\right] = 1/5, \tag{16}$$

where $f_Y(y) = 2\lambda_m \pi y \exp(-\lambda_m \pi y^2)$.

Proof: The distance between the typical user and its tagged MBS is Rayleigh distributed [30]. This implies $p_{in} = \int_0^\infty \left[1 - F_X(y)\right] f_Y(y)\, dy$, where $F_X(y) = \int_0^y f_X(x)\, dx$. Solving the integrals we get (16). ■

Lemma 2. *The probability that there are at least i D2D helpers inside B_{max} is given as*

$$p_{N_d}^{(i)} = 5(1 + 4\eta_d^{-1})^{-i} + \frac{10}{3}(1 + 6\eta_d^{-1})^{-i} - 8(1 + 5\eta_d^{-1})^{-i}. \tag{17}$$

[2]In our previous work in [32], we show that the maximal disk approximation is not accurate when the user is placed at a fixed distance from the MBS. In fact, a disk with the same area as the Voronoi cell better approximates the distance. However, in this case, we will show that when the distance Y between the requesting user and the MBS is random, the inscribed disk approximation accurately approximates the distance.

Proof: Given a disk B_{max} with radius $X = x$, the probability that there are at least i D2D helpers inside the disk is given as

$$\mathbb{P}\left[N_d \geq i | X = x\right] \;\; = \;\; 1 - \sum_{j=0}^{i-1} \frac{(\lambda_d \pi x^2)^j}{j!} \text{exp}\left(-\lambda_d \pi x^2\right) = 1 - \frac{\Gamma(i, \lambda_d \pi x^2)}{\Gamma(i)}.$$

Integrating over $X = x$ while ensuring $X > D$, we obtain

$$p_{N_d}^{(i)} = \int_0^\infty \left[\int_y^\infty \left[1 - \frac{\Gamma(i, \lambda_d \pi x^2)}{\Gamma(i)} \right] f_X(x)\, F_Y(x)\, dx \right] f_Y(y)\, dy, \tag{18}$$

where $F_Y(x) = \int_0^x f_Y(y)\, dy$. Simplification after evaluating the integrals and normalizing with p_{in} yields (17). ■

We now give the distribution of distance in the following Theorem.

Theorem 1. *The distribution of the distance between the typical user and its ith nearest D2D helper within the cell can be well approximated using the inscribed disk approximation for a Voronoi cell and is given as*

$$f_{R_i}(r) \quad = \quad \left[\int_0^\infty f_Y(y) \int_{a_1}^{a_2} f_{i,1}(r, y, x)\, f_X(x)\, F_Y(x) dx\, dy \;\; + \;\; f_{i,2}(r) \kappa(r) \right] \frac{1}{p_{in}\, p_{N_d}^{(i)}}, \tag{19}$$

where,

$$f_{i,1}(r) = \frac{\lambda_d^i}{\Gamma(i)} \nabla(r, y, x)^{i-1} \nabla^{'}(r, y, x) \, \text{exp}(-\lambda_d \nabla(r, y, x)), \tag{20}$$

$$f_{i,2}(r) = 2 \frac{(\lambda_d \pi)^i}{\Gamma(i)} r^{2i-1} \text{exp}(-\lambda_d \pi r^2), \tag{21}$$

$$\kappa(r) \;\; = \;\; \frac{\text{exp}\left(-4b\right)}{15} + b\sqrt{\pi} \left[\frac{\sqrt{6}}{9} \text{exp}\left(\frac{b}{6}\right) \text{erfc}\left(\frac{5\sqrt{6b}}{6}\right) - \frac{4\sqrt{5}}{25} \text{exp}\left(-\frac{4b}{5}\right) \text{erfc}\left(\frac{4\sqrt{5b}}{5}\right) \right], \tag{22}$$

where $b = \lambda_m \pi r^2$, $\nabla(r, y, x) = r^2 \arccos\left(\frac{\omega_1}{2y\, r}\right) + x^2 \arccos\left(\frac{\omega_2}{2y\, x}\right) - \frac{1}{2}\sqrt{4y^2x^2 - \omega_2^2}$, $\omega_1 = r^2 + y^2 - x^2$, $\omega_2 = x^2 + y^2 - r^2$, $\nabla^{'}(r, y, x)$ *is the derivative of* $\nabla(r, y, x)$ *with respect to* r, $a_1 = \max(y, r - y)$ *and* $a_2 = r + y$.

Proof: Please refer to Appendix A. ■

The expression in (19) is validated with network simulations in Section VI. Before further analysis, we develop some insights on the derived distance distribution in (19). We can write

$f_{R_i} = T_1 + T_2$, where $T_1 = (p_{in}\, p_{N_d}^{(i)})^{-1} \int_0^{\infty} \int_{a_1}^{a_2} f_{i,1}(r, y, x)\, f_X(x)\, F_Y(x) dx\, f_Y(y) dy$ and $T_2 = (p_{in}\, p_{N_d}^{(i)})^{-1} f_{i,2}(r) \kappa(r)$. We wish to see how the density of MBSs impacts T_1 and T_2 and in turn f_{R_i}.

Corollary 2. *For sparse networks, i.e. when $\lambda_m \to 0 (\eta_d \to \infty)$, $f_{R_i}(r)$ reduces to the distribution of distance to the unconstrained nearest D2D helper and is given by (21).*

Proof: Referring to Appendix A, we see that when $\lambda_m \to 0$, $x \gg r$ and $b(o, r)$ almost surely lies inside B_{max}. This in turn means $T_1 \to 0$. However, as $\lambda_m \to 0$, we see from (22) and (17) that $\kappa(r) = 1/15$ and $p_{N_d}^{(i)} = 1/3$. As $p_{in} = 1/5$ is fixed, T_2 reduces to $f_{i,2}(r)$. ■

Fig. 5 reinforces the result in Cor. 2. We compare (19) with the unconstrained ith nearest neighbor distribution [33]. We see that when the network is sparse, the term T_2 dominates $f_{R_i}(r)$ and the distribution of the distance to the ith nearest neighbor essentially approaches that of unconstrained case. This conclusion can be intuitively explained as we would expect that for very large cell sizes, the ith nearest D2D helper will reside in the same macrocell. However, as the MBS density increases, T_1 begins to increase and cannot be ignored. That is when (19) begins to significantly deviate from (21).

V. Performance Analysis under NS and US schemes

To assess the performance of cellular networks enhanced with coordinated D2D communication, we define the following quality-of-service (QoS) parameters.

A. Overall coverage probability

The typical user is in coverage in cellular mode when the received signal to interference and noise ratio (SINR) is greater than a certain modulation dependent decoding threshold τ_m. This is mathematically characterized as

$$\Gamma_m = \mathbb{P}\left[SINR_m \geq \tau_m\right].$$

Similarly, in D2D mode, when the user is served by its ith nearest D2D helper, the coverage probability is written as

$$\Gamma_{d,i} = \mathbb{P}\left[SINR_{d,i} \geq \tau_d\right],$$

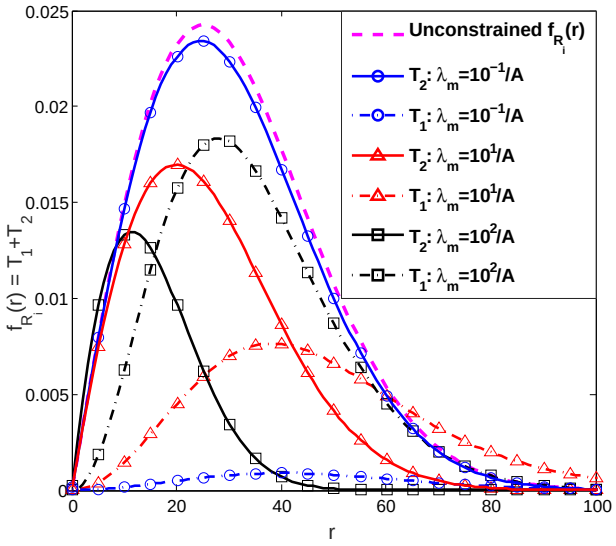

Figure 5: Effect of varying λ_m on T_1 and T_2: $i = 1, \lambda_d = 200/A, A = \pi 500^2$.

where τ_d is the SINR threshold in D2D mode. We define the overall coverage probability $\Gamma_{\Pi}^{(k)}(c)$ of an arbitrary user requesting content c by the following expression

$$\Gamma_{\Pi}^{(k)}(c) = (1 - p_{d,\Pi}^{(k)}(c))\Gamma_m + p_{d,\Pi}^{(k)}(c)\Gamma_{d,\Pi}^{(k)}(c), \tag{23}$$

where $\Gamma_{d,\Pi}^{(k)}(c)$ is the probability of coverage in D2D mode for a given k, content request c and D2D helper selection scheme $\Pi = \{NS, US\}$. Here, $p_{d,\Pi}^{(k)}(c)$ and $\left(1 - p_{d,\Pi}^{(k)}(c)\right)$ are the probabilities for D2D and cellular modes respectively.

Our first step is to obtain the D2D and cellular coverage probabilities of a typical link. When the typical user is operating in cellular mode, we have from [30]

$$\Gamma_m = \pi\lambda_m \int_0^{\infty} \exp\left(-\pi\lambda_m \nu \left(1 + \delta_m(s_m, \alpha)\right) - \frac{\tau_m \sigma^2}{P_m}\nu^{\alpha/2}\right), \tag{24}$$

where Γ_m is the cellular coverage probability, $s_m = \tau_m \nu^{\alpha}$ and $\delta_m(s_m, \alpha) = \tau_m^{2/\alpha} \int_{\tau_m^{-2/\alpha}} (1 + u^{\alpha/2}) du$.

Proposition 2. *Given that the typical user is served in D2D mode, the probability of coverage under the NS and US schemes can be expressed as*

$$\Gamma_{d,\Pi}^{(k)}(c) = \frac{\sum_{i=1}^{k} p_{d,\Pi}^{(k)}(i,c)\Gamma_{d,i}}{\sum_{i=1}^{k} p_{d,\Pi}^{(k)}(i,c)}, \ \Pi = \{NS, US\}, \tag{25}$$

where $\Gamma_{d,i}$ is the coverage probability when the typical user is served by the ith nearest D2D helper and is given as

$$\Gamma_{d,i} \approx \int_{r=0}^{\infty} \exp\left(-2\pi \frac{s_d \tilde{\lambda}_m \delta_d(s_d,\alpha)}{(\alpha-2)}\right) \exp\left(-s_d \frac{\sigma^2}{P_d}\right) f_{R_i}(r)\, dr \tag{26}$$

where $s_d = \tau_d r^{\alpha}$, $\delta_D(s,\alpha) = \mathbb{E}_Q\left[q^{-(\alpha-2)}{}_2F_1\,(1,\bar{\alpha};1+\bar{\alpha};-sq^{-\alpha})\right]$, $\bar{\alpha} = 1-2/\alpha$ and $f_Q(q) = 2\pi\tilde{\lambda}_M q \exp(-\tilde{\lambda}_M \pi q^2)$.

Proof: Please refer to Appendix B ■

B. Average Rate

Using a similar exposition as in the previous subsection, we express the average rate $T_{\Pi}^{(k)}(c)$ experienced by an arbitrary user requesting content c under the NS and US schemes as

$$T_{\Pi}^{(k)}(c) = \left(1 - p_{d,\Pi}^{(k)}(c)\right) \overline{R_{m,\Pi}}(c) + p_{d,\Pi}^{(k)}(c) \overline{R_{d,\Pi}}(c) \text{ bps}, \tag{27}$$

where $p_{d,\Pi}^{(k)}(c)$ and $\left(1 - p_{d,\Pi}^{(k)}(c)\right)$ are the probabilities for D2D and cellular communication and $\overline{R_{m,\Pi}}(c)$ and $\overline{R_{d,\Pi}}(c)$ are respectively the average cellular and D2D rates.

Proposition 3. *The average rate experienced by an arbitrary user requesting content 'c' in D2D mode under NS and US schemes is expressed as*

$$\overline{R_{d,\Pi}^{(k)}}(c) = W_d \gamma\left(\eta_{u_{d,\Pi}}\right) \frac{\sum_{i=1}^{k} p_{d,\Pi}^{(k)}(i,c) R_{d,i}}{p_{d,\Pi}^{(k)}(c)}, \tag{28}$$

$$R_{d,i} = \mathbb{E}\left[\log_2(1 + SINR_{d,i})\right], \tag{29}$$

where $\Pi = \{NS, US\}$, $\gamma(a) = (1 - \exp(-a))/a$, W_d is the bandwidth reserved for D2D communication and $\eta_{u_{d,\Pi}} = \lambda_{u_{d,\Pi}}/\lambda_m$. Here, $\lambda_{u_{d,\Pi}} = \lambda_u \rho \sum_{c=1}^{L} c^{-\zeta} p_{d,\Pi}^{(k)}(c)$ is the average density of users operating in D2D mode.

Proof: The average D2D rate can be written as

$$\overline{R_{d,\Pi}^{(k)}}(c) = \mathbb{E}\left[\frac{W_d}{N_{u_{d,\Pi}}}\right] R_{d,\Pi}^{(k)}(c), \tag{30}$$

where $R_{d,\Pi}^{(k)}(c)$ is the average capacity of the link when content c is requested. It is obtained by taking the expectation of (29), which is the average ergodic capacity of a D2D link between

an arbitrary user and its ith nearest D2D helper. $\mathbb{E}\left[W_d/N_{u_{d,\Pi}}\right]$ is the average bandwidth available for the communication on a D2D link where $N_{u_{d,\Pi}} \sim$ Poisson $(\eta_{u_{d,\Pi}})$ is the number of simultaneously active users in D2D mode inside the cell[3]. Hence,

$$\begin{aligned}\mathbb{E}\left[1/N_{u_{d,\Pi}}\right] &= \sum_{n=1}^{\infty} \frac{1}{n} \frac{(\eta_{u_{d,\Pi}})^{n-1}}{(n-1)!} \exp\left(-\eta_{u_{d,\Pi}}\right), \\ &= \eta_{u_{d,\Pi}}^{-1}\left(1-\exp\left(-\eta_{u_{d,\Pi}}\right)\right). \end{aligned} \tag{31}$$

where the summation starts from $n=1$ to account for the presence of the user under consideration. ■

Proposition 4. *The average rate experienced by an arbitrary user requesting content 'c' in cellular mode under NS and US schemes is expressed as*

$$\overline{R_{m,\Pi}^{(k)}}(c) = W_m \hat{R}_m \gamma\left(\eta_{u_{m,\Pi}}\right) \tag{32}$$

where $\hat{R}_m(c) = R_m\left(\mathbb{I}_{c\leq C_m} + \beta\,\mathbb{I}_{c>C_m}\right)$ *is the average capacity of cellular links,* $\mathbb{I}_{c\leq C_m}$ *and* $\mathbb{I}_{c>C_m}$ *are respectively the cellular hit and miss rates,* $R_m = \mathbb{E}\left[\log_2(1+SINR_m)\right]$ *,* β *is the backhaul delay coefficienct,* W_m *is the cellular bandwidth, and* $\eta_{u_{m,\Pi}} = \lambda_{u_{m,\Pi}}/\lambda_m$ *with* $\lambda_{u_{m,\Pi}} = \lambda_u(1-\rho\sum_{c=1}^{L} c^{-\zeta} p_{d,\Pi}^{(k)}(c))$.

Proof: The proof is on the similar lines as Proposition 3 with the exception that the average density of cellular users is $\lambda_u - \lambda_{u_{d,\Pi}}$, i.e. all the users which are not operating in D2D mode are shifted to cellular mode. Furthermore, when the requested content is not present in the MBS cache, the average rate of the cellular link is reduced by a factor β, which accounts for the delay introduced by fetching the content from backhaul. ■

VI. Results and Discussion

In this section, we will give some key results and verify our analysis with Monte Carlo simulations. For our simulation setup, the MBSs and D2D helpers are distributed according to HPPPs with intensities λ_m and λ_d respectively and the performance is measured at the origin.

[3]To simplify the analysis, we assume that the number of users in D2D mode is the same as the number of active D2D helpers. This might not be the case in reality as one helper can serve multiple users in its vicinity if they request the same file. With our analysis, such a situation will translate into the transmission of the same file by the same D2D helper but on a separate portion of the spectrum.

Parameter	Description	Value
α	Path loss exponent	4
$\lambda_m, \lambda_d, \lambda_u$	MBS, D2D helper and user density	$[10, 100, 200]/\pi 500^2$
ζ	Popularity skewness parameter	0.8
c, L	Requested content, Library size	1, 10^4
β	Backhaul delay coefficient	0.8
C_d, C_m	D2D and MBS cache sizes	20, 500
W_m, W_d	Cellular and D2D bandwidth	$[7, 3]$ MHz
P_m, P_d	Cellular and D2D transmit power	$[30, 23]$ dBm
τ_m, τ_d	Cellular and D2D SINR threshold	$[30, 30]$ dBm
σ^2	Noise power	-110 dBm

Table I: List of simulation parameters

We first validate the distribution of distance to the ith nearest D2D helper derived in Theorem 1 for various values of i. For the simulations, we ignore the realizations in which the number of D2D helpers is less than i in the typical cell. In case of the disk approximation, the realizations in which the typical user lies outside B_{max}, or there are less than i D2D helpers inside B_{max}, are all ignored. Fig. 6 shows that the disk approximation is very accurate, while the unconstrained nearest neighbor distribution in (21) does not encapsulate the behavior of the distance distribution and the deviations from the actual distribution become large as the value of i increases.

Fig. 7 validates our analysis of the probability of coverage $\Gamma_{d,i}$ when the typical user is being served by the ith nearest D2D helper ((26) in Theorem 2). We see that the disk approximation holds fairly accurately for all values of i. The slight deviation of the analysis using the disk approximation from the simulations using disk approximation is because of the equi-dense HPPP approximation for the D2D interferers. As expected, we see a decrease in $\Gamma_{d,i}$ with the increases in i for a fixed SINR threshold. This is because, as i increases, the distance between the transmitting D2D helper and the typical user increases, thereby aggravating the path loss. For comparison, we also plot the cellular coverage Γ_m given in (24). For a given SINR threshold, we see that

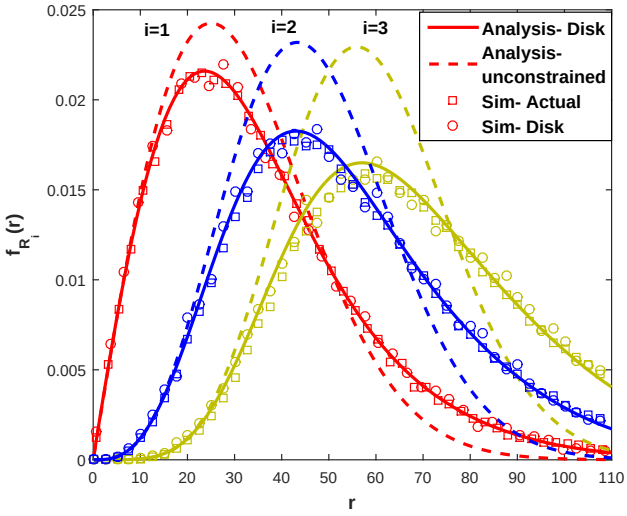

Figure 6: Distribution of the distance to the ith nearest D2D helper from the tagged user within the Voronoi cell, where $\lambda_m = 20/\pi 500^2$, and $\lambda_d = 200/\pi 500^2$.

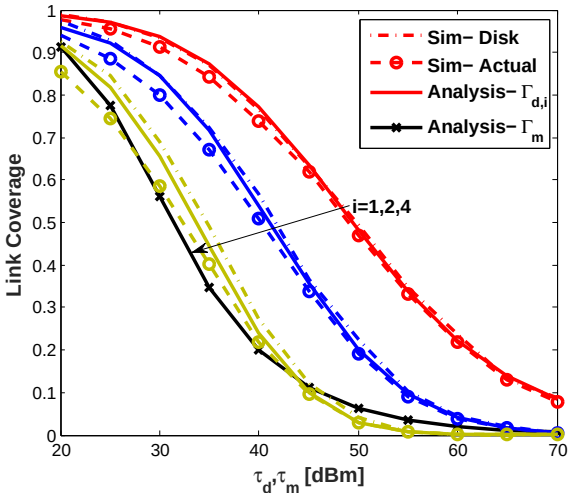

Figure 7: Probability of coverage when a typical user is served by the MBS or the ith nearest D2D helper.

small values of i result in a much better coverage for a D2D link compared to the cellular link.

Fig. 8 illustrates the probability of being in coverage in D2D mode. We also validate the D2D coverage probability $\Gamma^{(k)}_{d,\Pi}(c), \Pi = \{NS, US\}$ derived in Theorem 2 (25). For each simulation

trial, maximum k closest D2D helpers are first checked for content availability. The content availability ($c = 1$ in this case) is a Bernoulli event with probability $h_d(c)$. Out of the successful D2D helpers (if there are any), the helper is selected either uniformly (US scheme) or closest to the origin (NS scheme). We see that the D2D coverage probability for the NS scheme outperforms the US scheme. This is because in the US scheme, a D2D helper is uniformly selected out of the maximum k closest helpers, while the closest helper is given preference in the NS scheme.

The behavior of the D2D coverage probability $\Gamma_{d,\Pi}^{(k)}(c), \Pi = \{NS, US\}$ is further investigated when the value of k is changed. We can see from Fig. 9 that the increase in k adversely affects $\Gamma_{d,US}^{(k)}(c)$. However, the effect on $\Gamma_{d,NS}^{(k)}(c)$ is much less pronounced.

A. Performance Evaluation

We now study the performance metrics defined in Sec. V with respect to the two key parameters, namely, the number of candidate neighboring D2D helpers k and the requested content c. We first consider the overall coverage probability $\Gamma_{\Pi}^{(k)}(c), \Pi = \{NS, US\}$ given in (23). The simplified expressions for $\Gamma_{\Pi}^{(k)}(c)$ are presented in (33) and (34) using the upper bounds for $p_{\Pi}^{(k)}(i, c)$ from Corollary 1. In Fig. 10, the overall coverage probability for the US scheme $\Gamma_{US}^{(k)}(c)$ is seen to monotonically decrease with the increase in k, starting with a maximum value at $k_{US}^{*} = 1$. This is because, from Fig. 7 we see that the D2D link coverage $\Gamma_{d,i}$ decreases as i increases and even gets worse compared to the cellular link coverage Γ_m. As k increases in (33), the contribution of $\Gamma_{d,1}$ decreases in the second term corresponding to the coverage in D2D mode. Intuitively, this means that the MBS does not make an intelligent decision in the selection of the D2D helper and may select a helper farther from the requesting user for D2D communication. As the first term in (33) is independent of k, and $\Gamma_{d,i}$ is a decreasing function in i, (33) is always maximized when $k_{US}^{*} = 1$. On the contrary, the plots for $\Gamma_{NS}^{(k)}(c)$ reveal

---

$$\Gamma_{US}^{(k)}(c) \approx \left[1 - \rho c^{-\zeta}\right]^{C_d} \Gamma_m + \frac{1}{k}\left(1 - \left[1 - \rho c^{-\zeta}\right]^{C_d}\right) \sum_{i=1}^{k} \Gamma_{d,i} \tag{33}$$

$$\Gamma_{NS}^{(k)}(c) \approx \left[1 - \rho c^{-\zeta}\right]^{kC_d} \Gamma_m + \left(1 - \left[1 - \rho c^{-\zeta}\right]^{C_d}\right) \sum_{i=1}^{k} \left[1 - \rho c^{-\zeta}\right]^{(i-1)C_d} \Gamma_{d,i} \tag{34}$$

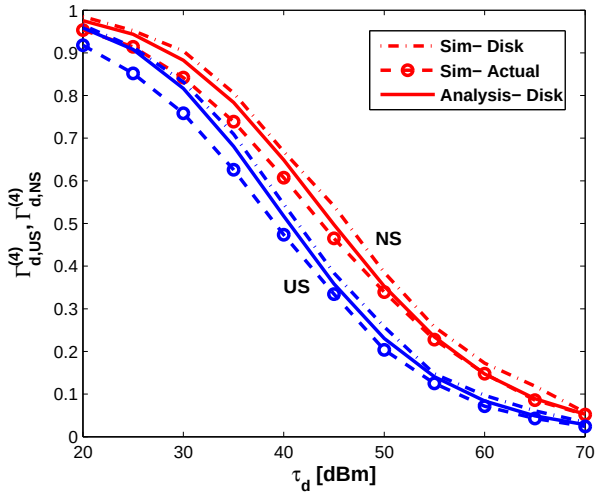

Figure 8: Coverage probability in D2D mode under the NS and US schemes.

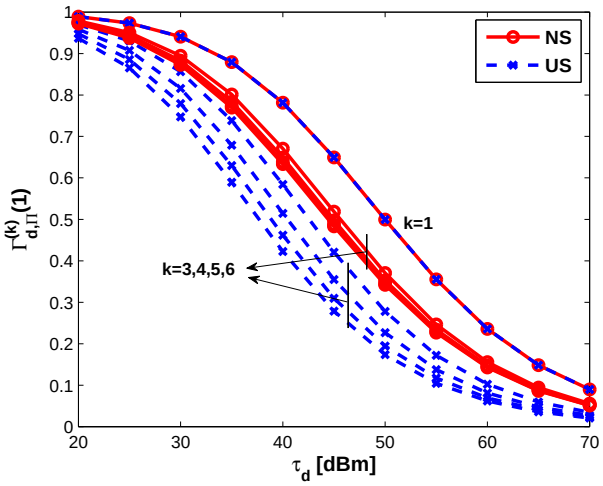

Figure 9: D2D coverage for various values of k (increasing to the left).

an interesting trade off in the selection of k to maximize the overall coverage. We see that for a given SINR threshold (and also $\tau_d = \tau_m$), there exists an optimal value of $k = k^*_{NS}$, which maximizes $\Gamma^{(k)}_{NS}(c)$ (shown by the dotted line). The explanation for this phenomenon is given as follows. We see that as k is increased, the probability of cellular mode is decreased as the term $\left[1 - \rho c^{-\zeta}\right]^{kC_d}$ premultiplied with Γ_m in (34) decreases. Initially, $\Gamma^{(k)}_{NS}(c)$ rises with the increase in k and attains a maximum value at k^*_{NS}, but with further increase in k, the coverage $\Gamma_{d,i}$

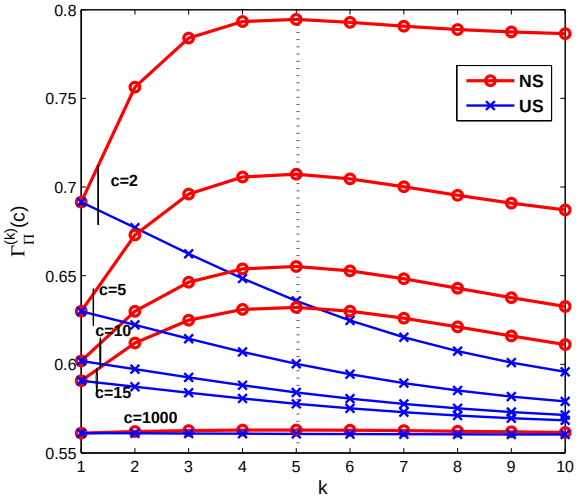

Figure 10: Effect of increasing k on the overall coverage probability for various content requests.

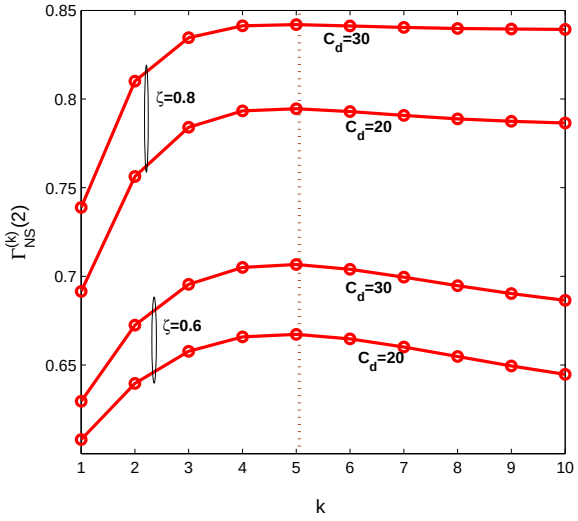

Figure 11: Effect of D2D caching parameters on k_{NS}^{*}.

with the activated D2D links is no longer better than the cellular coverage as already seen from Fig. 7, hence, $\Gamma_{NS}^{(k)}(c)$ begins to drop. We observe that as the requested content c becomes less popular, both $p_{NS}^{(k)}(c)$ and $p_{US}^{(k)}(c)$ drop, and for the least popular requested content $\Gamma_{\Pi}^{(k)}(c) \to \Gamma_m$ as $h_d(c) \to 0$ implying that the requesting user can only be served in cellular mode. It can also be seen that varying c does not affect the optimal value k_{NS}^{*}. In Fig. 11, we also observe the

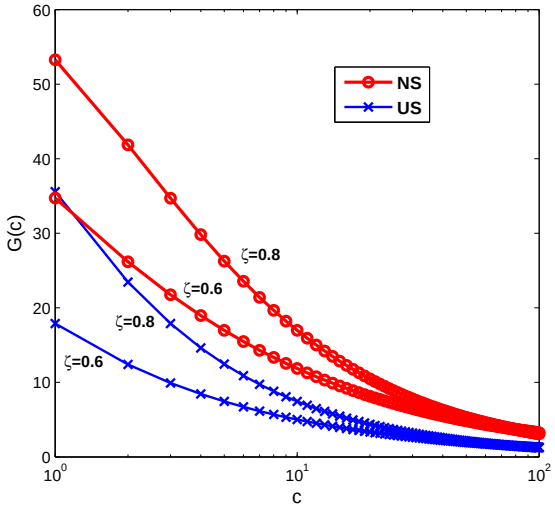

Figure 12: Percentage maximum gain in the overall coverage with coordinated D2D under NS and US schemes.

effect of the other crucial D2D caching parameters, ζ and C_d on $\Gamma_{NS}^{(k)}(c)$. We see that k_{NS}^{*} is also resilient to the changes in ζ and C_d, but the maximum value of the overall coverage $\Gamma_{NS}^{(k)}(c)$ increases with the increase in ζ and C_d. This is due to the fact that popular content c or higher values of ζ and C_d all translate into a higher probability of being served by the ith nearest D2D helper as $p_{\Pi}^{(k)}(i,c)$ increases $\forall i = \{1,..,k\}$, but these parameters do not affect the link quality (Γ_m and $\Gamma_{d,i}$). Therefore, k_{NS}^{*} is independent of the caching parameters.

To better visualize the improvement in coverage compared to the conventional cellular network scenario, we compute the gain in the overall coverage probability. It is the percentage difference

$$T_{US}^{(k)}(c) \approx \left[1-\rho c^{-\zeta}\right]^{C_d} W_m \gamma\left(\eta_{u_{m,US}}\right) \hat{R}_m(c) + \frac{W_d}{k} \gamma\left(\eta_{u_{d,US}}\right) \left(1-\left[1-\rho c^{-\zeta}\right]^{C_d}\right) \sum_{i=1}^{k} R_{d,i} \quad (35)$$

$$\begin{aligned} T_{NS}^{(k)}(c) \quad \approx \quad & \left[1-\rho c^{-\zeta}\right]^{kC_d} W_m \gamma\left(\eta_{u_{m,NS}}\right) \hat{R}_m(c) \\ & + W_d \gamma\left(\eta_{u_{d,NS}}\right) \left(1-\left[1-\rho c^{-\zeta}\right]^{C_d}\right) \sum_{i=1}^{k} \left[1-\rho c^{-\zeta}\right]^{(i-1)C_d} R_{d,i} \end{aligned} \quad (36)$$

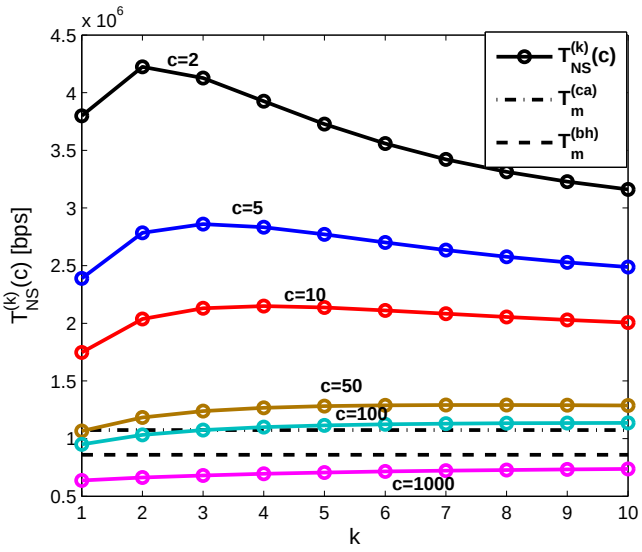

Figure 13: Effect of increasing k on the average rate experienced by an arbitrary user for various content requests.

between the maximum attainable overall coverage probability under the NS and US schemes $\Gamma_{\Pi}^{(k_{\Pi}^*)}(c), \Pi = \{NS, US\}$ and the conventional cellular coverage probability. It is given as

$$G(c) = \frac{\Gamma_{\Pi}^{(k_{\Pi}^*)}(c) - \Gamma_m}{\Gamma_m} \times 100\%.$$

Figure 12 shows that for popular content requests and skewed popularity distribution, more than 50% better coverage can be obtained with the NS scheme compared to the conventional scenario. The US scheme does not perform as good as the NS scheme, but it yields sufficient gains (35% at best under the given network setting).

We will now focus on the analysis of average rate experienced by the user in the US and NS schemes to gain some more useful insights on the design of cellular networks enabled with coordinated D2D communication. The simplified expressions for $T_{US}^{(k)}(c)$ and $T_{NS}^{(k)}(c)$ using Corollary 1 are given in (35) and (36) respectively. For the average rate with the US scheme, we see from (35) that $T_{US}^{(k)}(c)$ exhibits the same behavior as $\Gamma_{US}^{(k)}(c)$ the increase in k reduces the average rate in D2D mode because D2D helpers located farther from the requesting user are selected with the probability equal to the nearest helpers. Hence, $\Gamma_{US}^{(k)}(c)$ is only maximized when $k = k_{US}^* = 1$.

To visualize when maximum gains can be harnessed with the NS scheme, we plot the $\Gamma_{NS}^{(k)}(c)$ in Fig. 13 and compare it with the rates experienced by the user in a cellular only network. The rate experienced by the user in a cellular network where the MBS is equipped with caching capability is given as

$$T_m^{(ca)} = (W_m + W_d)\gamma\left(\eta_u\right) R_m. \tag{37}$$

Notice that all of the bandwidth $W_d + W_c$ is used for cellular communication and $\eta_u = \lambda_u/\lambda_m$ as all the requesting users in the cell share the cellular link capacity. When there is no caching at the MBS, the rate is reduced by a fraction β due to the delay introduced by the backhaul communication and is given as

$$T_m^{(bh)} = \beta T_m^{(ca)}. \tag{38}$$

The following conclusions can be drawn from Fig. 13. Coordinated D2D communication with content centric mode selection greatly enhances data rates compared to cellular only scenarios when popular contents are requested. This is because we know that for small c, $h_d(c)$ (and in turn $p_{NS}^{(k)}(i,c)$) increases implying that more users can be served by their nearest D2D helper in D2D mode. For least popular contents, the rate experienced by the requesting user is severely degraded and is even lower than the cellular only scenario. This is because, $h_d(c) \to 0$ and the user is pushed to communicate in cellular band W_m, which is less than the total bandwidth $W_m + W_d$ of the cellular only scenario. Yet again, there exists a trade off in the selection of the number of neighboring D2D helpers k which maximizes the average throughput experienced by an arbitrary user. The existence of the optimal value of $k = k_{NS}^*$ for $T_{NS}^{(k)}(c)$ follows the same reasoning as $\Gamma_{NS}^{(k)}(c)$, as $R_{d,i}$ follows the same trend as $\Gamma_{d,i}$ and is decreasing in i. However, Unlike the $\Gamma_{NS}^{(k)}(c)$, this value of $k = k_{NS}^*$ does vary with the changes in c and increases as c increases. This is because, as we have from Proposition 3

$$\begin{aligned}
\eta_{u_{d,NS}} &= \frac{\lambda_u}{\lambda_m}\left[\rho\sum_{c=1}^{L} c^{-\zeta} p_{d,NS}^{(k)}(c)\right] \\
&= \frac{\lambda_u}{\lambda_m}\left[1 - \rho\sum_{c=1}^{L} c^{-\zeta}[1-\rho c^{-\zeta}]^{kC_d}\right],
\end{aligned}$$

where $\gamma\left(\eta_{u_{d,NS}}\right) = \eta_{u_{d,\Pi}}^{-1}\left(1-\exp\left(-\eta_{u_{d,\Pi}}\right)\right)$ is a decreasing function in k. This means that more users are offloaded from cellular to D2D mode as k increases and the available bandwidth $W_d\gamma\left(\eta_{u_{d,NS}}\right)$ for a user in D2D mode decreases. When $k \to \infty$, $\gamma\left(\eta_{u_{d,NS}}\right) \to \gamma\left(\eta_u\right)$ implying

that all the requesting users are served in D2D mode. We know that as c increases, then the term $1-\left[1-\rho c^{-\zeta}\right]^{C_d}$ decreases in (36) and the D2D rate decreases. To effectively utilize the D2D bandwidth W_d, more users need to be activated in D2D mode and hence, k_{NS}^{*} increases.

VII. Conclusion

In this paper, we presented a novel framework for the analysis of cache-enabled cellular networks with coordinated D2D communication. The arbitrary user requesting a particular content is offloaded to communicate with one of its k neighboring D2D helpers within the cell based on the content availability and helper selection schemes. We derived the distribution of the distance between the user and its ith nearest D2D helper within the cell using disk cell approximation, which is shown to be fairly accurate. We obtained the probabilities for being served in cellular and D2D modes and the coverage and data rates experienced by the user in both these modes. With the help of our analysis, we showed that the information-centric offloading with coordinated D2D results in high performance gain. However, to maximize the performance, the number of candidate D2D helpers k has to be carefully tuned.

Appendix A
Proof of Theorem 1

The probability that the distance between the requesting user and the ith nearest D2D helper within the cell is at least r is the probability that there are exactly $i-1$ helpers inside the region $\mathcal{A}$. It can be expressed as

$$1-F_{R_i|X=x,X>D,N_d\geq i}(r)=\frac{\left(\lambda_d\mathcal{A}\right)^{i-1}}{(i-1)!}\exp\left(-\lambda_d\mathcal{A}\right), \tag{39}$$

where $\mathcal{A}$ is the area of intersection between B_m and $b(o,r)$. As shown in Fig. 14, this area can be divided into two regimes given as follows.

- Regime 1 - When $b(o,r)$ partly overlaps B_m, i.e. $x-y<r<x+y$. The overlapping area $\mathcal{A}$ in this case can be written as [34]

$$\nabla(r,y,x) \;=\; r^2\arccos\left(\frac{\omega_1}{2y\,r}\right)+x^2\arccos\left(\frac{\omega_2}{2y\,x}\right)-\frac{1}{2}\sqrt{4y^2x^2-\omega_2^2}, \tag{40}$$

  where $\omega_1=r^2+y^2-x^2$ and $\omega_2=x^2+y-r^2$.

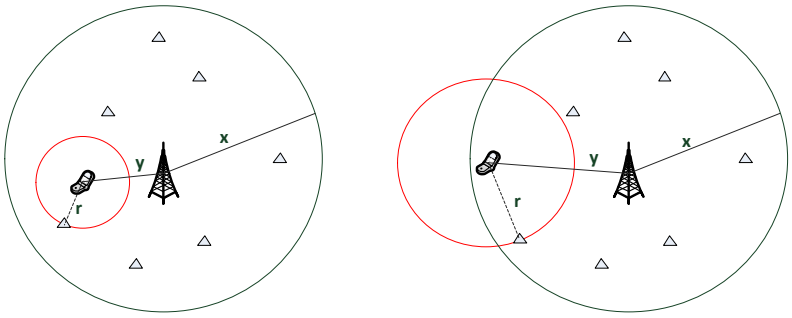

(a) (b)

Figure 14: Distance to the nearest D2D neighbor within the circular Voronoi cell: (a) when $b(o,r)$ is inside B_{max}, (b) when $b(o,r)$ partly overlaps B_{max}.

- Regime 2 - When $b(o,r)$ lies inside B_m i.e. $0 < r < x - y$. The overlapping area in this case is straightforward and is given as $\mathcal{A} = \pi r^2$.

Differentiating $F_{R_i|X=x,X>D,N_d\geq i}(r)$ in (39) with respect to r gives (20) and (21) for regimes 1 and 2 respectively. The unconditional distance distribution $f_{R_i}(r)$ in (19) is obtained by averaging over X and Y, where $X > Y$ and $N_d \geq i$.

APPENDIX B
PROOF OF PROPOSITION 2

The probability of coverage for the typical user served by the ith nearest D2D helper can be expressed as

$$\Gamma_{d,i} \;=\; \mathbb{P}\left\{\frac{h_i\, r^{-\alpha}}{\sigma^2/P_d + I_d} > \tau_d\right\} \tag{41}$$

where $I_d = \sum_{z_j \in \Phi_d^{int}} g_j\, z_j^{-\alpha}$ is the inter-cell interference from other active D2D helpers, which is the sum of powers from the active D2D helpers constituting Φ_d^{int}. Here, z_j is the distance of the the interfering D2D helper from the typical user and g_j is the channel power for the interfering link j. Because of the exponentially distributed channel power h_i in (41), we get

$$\Gamma_{d,i} = \mathbb{E}_{R_i}\left[\exp\left(-s_d\sigma^2/P_d\right)\mathcal{L}_{I_d}\left(s_d\right)\right], \tag{42}$$

where $s_d = \tau_d r^\alpha$ and $\mathcal{L}_{I_d}\left(s_d\right) = \mathbb{E}_{I_d}\left[\exp\left(-s_d I_d\right)\right]$ is the Laplace transform of D2D interference. Because only one D2D helper can be active at one channel in a given macrocell, we employ a key

assumption that Φ_d^{int} is a HPPP with intensity $\tilde{\lambda}_m = p_{int} \times \lambda_m$ [4]. Here, $p_{int} = 1-(1+3.5^{-1}\eta_d)^{-3.5}$ is the probability that at least one interfering D2D helper is present in a cell. $\mathcal{L}_{I_d}(s_d)$ can then be presented as

$$\begin{aligned} \mathcal{L}_{I_d}(s_d) &= \mathbb{E}\left[\exp\left(-s_d \sum_{\mathbf{z}_j \in \Theta_d} g_j \, z_j^{-\alpha}\right)\right] \\ &\overset{(a)}{=} \mathbb{E}_Q\left[\exp\left(-2\pi\tilde{\lambda}_m \int_q^{\infty} \frac{\nu}{1+s_d^{-1}\nu^{\alpha}}\, d\nu\right)\right] \end{aligned} \tag{43}$$

where (a) follows from the generating functional of a HPPP and the exponential distribution of the channel power g. The lower limit of the integral in (43) represents the guard zone. Notice that the lower limit q in this case is governed by the nearest active D2D interferer, where $f_Q(q) = 2\pi\tilde{\lambda}_m q \exp(-\tilde{\lambda}_m \pi q^2)$ because of the equi-dense HPPP approximation. As $\tilde{\lambda}_M$ is quite small, we can apply Jensen's inequality to achieve a tight bound for (43)

$$\mathcal{L}_{I_d}(s_d) \approx \exp\left(-2\pi\tilde{\lambda}_m \mathbb{E}_Q\left[\int_q^{\infty} \frac{\nu}{1+s_d^{-1}\nu^{\alpha}}\, d\nu\right]\right). \tag{44}$$

Substituting (44) into (42) gives (26).

The overall D2D coverage probability for NS and US schemes and a particular content request in (25) is obtained by taking expectation over i and by conditioning over the probability of D2D mode.

REFERENCES

[1] E. Bastug, M. Bennis, and M. Debbah, "Living on the Edge: The Role of Proactive Caching in 5G Wireless Networks," *IEEE Communications Magazine*, vol. 52, no. 8, pp. 82–89, 2014.

[2] S. Woo, E. Jeong, S. Park, J. Lee, S. Ihm, and K. Park, "Comparison of Caching Strategies in Modern Cellular Backhaul Networks," in *Proceeding of the 11th annual international conference on Mobile systems, applications, and services*. ACM, 2013, pp. 319–332.

[3] X. Lin, J. Andrews, A. Ghosh, and R. Ratasuk, "An Overview of 3GPP Device-to-Device Proximity Services," *IEEE Communications Magazine*, vol. 52, no. 4, pp. 40–48, 2014.

[4] F. Malandrino, C. Casetti, and C.-F. Chiasserini, "Toward D2D-Enhanced Heterogeneous Networks," *IEEE Communications Magazine*, vol. 52, no. 11, pp. 94–100, 2014.

[4]The equi-dense HPPP assumptions ignores the correlations due to the position of helpers inside a cell, but is more tractable. [20]

[5] G. Fodor, E. Dahlman, G. Mildh, S. Parkvall, N. Reider, G. Miklós, and Z. Turányi, "Design Aspects of Network Assisted Device-to-Device Communications," *IEEE Communications Magazine*, vol. 50, no. 3, pp. 170–177, 2012.

[6] A. Asadi, Q. Wang, and V. Mancuso, "A Survey on Device-to-Device Communication In Cellular Networks," *IEEE Communications Surveys & Tutorials*, vol. 16, no. 4, pp. 1801–1819, 2014.

[7] M. Haenggi, *Stochastic Geometry for Wireless Networks*. Cambridge University Press, 2012.

[8] M. Ji, G. Caire, and A. Molisch, "Fundamental limits of caching in wireless d2d networks," *IEEE Transactions on Information Theory*, vol. 62, no. 2, pp. 849 – 869, 2014.

[9] M. Ji, G. Caire, and A. F. Molisch, "Wireless device-to-device caching networks: Basic principles and system performance," *IEEE Journal on Selected Areas in Communications*, vol. 34, no. 1, pp. 176–189, 2016.

[10] N. Golrezaei, P. Mansourifard, A. F. Molisch, and A. G. Dimakis, "Base-station assisted device-to-device communications for high-throughput wireless video networks," *IEEE Transactions on Wireless Communications*, vol. 13, no. 7, pp. 3665–3676, 2014.

[11] B. Perabathini, E. Bastug, M. Kountouris, M. Debbah, and A. Conte, "Caching at the Edge: a Green Perspective for 5G Networks," *CoRR*, vol. abs/1503.05365, 2015. [Online]. Available: http://arxiv.org/abs/1503.05365

[12] S. A. R. Zaidi, M. Ghogho, and D. C. McLernon, "Information Centric Modeling for Two-tier Cache Enabled Cellular Networks," *IEEE International Conference on Communications (ICC)*, 2015.

[13] S. Tamoor-ul Hassan, M. Bennis, P. H. Nardelli, and M. Latva-Aho, "Modeling and Analysis of Content Caching in Wireless Small Cell Networks," *arXiv preprint arXiv:1507.00182*, 2015.

[14] E. Bastug, M. Bennis, and M. Debbah, "Cache-Enabled Small Cell Networks: Modeling and Tradeoffs," in *11th International Symposium on Wireless Communications Systems (ISWCS)*. IEEE, 2014, pp. 649–653.

[15] M. Afshang, H. S. Dhillon, and P. H. J. Chong, "Fundamentals of cluster-centric content placement in cache-enabled device-to-device networks," *arXiv preprint arXiv:1509.04747*, 2015.

[16] Z. Chen, J. Lee, T. Q. Quek, and M. Kountouris, "Cooperative caching and transmission design in cluster-centric small cell networks," *arXiv preprint arXiv:1601.00321*, 2016.

[17] M. Afshang, H. S. Dhillon, and P. H. J. Chong, "Modeling and Performance Analysis of Clustered Device-to-Device Networks," *arXiv preprint arXiv:1508.02668*, 2015.

[18] A. Altieri, P. Piantanida, L. R. Vega, and C. G. Galarza, "On Fundamental Trade-offs of Device-to-Device Communications in Large Wireless Networks," *CoRR*, vol. abs/1405.2295, 2014. [Online]. Available: http://arxiv.org/abs/1405.2295

[19] X. Lin, J. G. Andrews, and A. Ghosh, "Spectrum Sharing for Device-to-Device Communication in Cellular Networks," *IEEE Transactions on Wireless Communications*, vol. 13, no. 12, pp. 6727–6740, 2014.

[20] H. ElSawy, E. Hossain, and M.-S. Alouini, "Analytical Modeling of Mode Selection and Power Control for Underlay d2d Communication in Cellular Networks," *IEEE Transactions on Communications*, vol. 62, no. 11, pp. 4147–4161, 2014.

[21] U. Niesen and M. A. Maddah-Ali, "Coded Caching for Delay-Sensitive Content," *arXiv preprint arXiv:1407.4489*, 2014.

[22] A. Dabirmoghaddam, M. M. Barijough, and J. Garcia-Luna-Aceves, "Understanding Optimal Caching and Opportunistic Caching at the Edge of Information-Centric Networks," in *Proceedings of the 1st international conference on Information-centric networking*. ACM, 2014, pp. 47–56.

[23] E. Baştuğ, M. Bennis, and M. Debbah, "A Transfer Learning Approach for Cache-Enabled Wireless Networks," *arXiv preprint arXiv:1503.05448*, 2015.

[24] C. Fricker, P. Robert, J. Roberts, and N. Sbihi, "Impact of Traffic Mix on Caching Performance in a Content-Centric

Network," in *IEEE Conference on Computer Communications Workshops (INFOCOM WKSHPS)*. IEEE, 2012, pp. 310–315.

[25] B. Blaszczyszyn and A. Giovanidis, "Optimal geographic caching in cellular networks," in *IEEE International Conference on Communications (ICC)*. IEEE, 2015, pp. 3358–3363.

[26] K. Avrachenkov, X. Bai, and J. Goseling, "Optimization of caching devices with geometric constraints," *arXiv preprint arXiv:1602.03635*, 2016.

[27] D. Liu and C. Yang, "Energy Efficiency of Downlink Networks with Caching at Base Stations," *CoRR*, vol. abs/1505.06615, 2015. [Online]. Available: http://arxiv.org/abs/1505.06615

[28] D. Stoyan, W. S. Kendall, J. Mecke, and L. Ruschendorf, *Stochastic geometry and its applications*. Wiley New York, 1987, vol. 2.

[29] S. M. Yu and S.-L. Kim, "Downlink capacity and base station density in cellular networks," in *11th International Symposium on Modeling & Optimization in Mobile, Ad Hoc & Wireless Networks (WiOpt)*. IEEE, 2013, pp. 119–124.

[30] J. G. Andrews, F. Baccelli, and R. K. Ganti, "A tractable approach to coverage and rate in cellular networks," *IEEE Transactions on Communications*, vol. 59, no. 11, pp. 3122–3134, 2011.

[31] S. Foss and S. Zuyev, "On a Voronoi Aggregative Process Related to a Bivariate Poisson Process," *Advances in Applied Probability*, pp. 965–981, 1996.

[32] A. Afzal, S. A. R. Zaidi, M. Ghogho, and D. C. McLernon, "On the analysis of cellular networks with caching and coordinated device-to-device communication," *IEEE International Conference on Communications (ICC)*, 2016.

[33] D. Moltchanov, "Survey paper: Distance distributions in random networks," *Ad Hoc Networks*, vol. 10, no. 6, pp. 1146–1166, 2012.

[34] E. W. Weisstein, "Circle-circle intersection," 2003.